The interaction of superfluid vortex filaments with a normal fluid channel flow

By D. C. Samuels

Vortex filaments in superfluids such as helium II may provide new insights into very high Reynolds number flows. We simulate the behavior of a superfluid vortex ring interacting with a normal fluid shear flow, specifically channel flow. The vortex ring evolves into a stable horseshoe configuration which propagates without further change of form. In this simulation, we demonstrate a boundary layer behavior in a superfluid through the coupling of the superfluid and the normal fluid.

1. Motivation and objectives

Superfluids such as helium II provide a true vortex filament system which can be explored both experimentally and numerically. Vorticity in helium II is confined to filaments with a measured radius of approximately one Å. These superfluid vortices may be treated as one-dimensional singularities to a good approximation for all length scales greater than $\sim 10^2 Å$. The circulation about each vortex filament is quantized in units of h/m where h is Planck's constant and m is the mass of the helium atom. Due to energy considerations, only a single quantum of circulation is present around each vortex; therefore, we have the circulation $\Gamma = h/m$ for all helium II vortices. For a detailed discussion of vortices in helium II, see Glaberson and Donnelly (1986).

The motion of a vortex filament in the rest frame of the superfluid is determined from the Biot-Savart law,

$$\vec{v}(\vec{r}) = \frac{\Gamma}{4\pi} \int \frac{(\vec{s} - \vec{r}) \otimes d\vec{s}}{|\vec{s} - \vec{r}|^3} \tag{1}$$

where the integral is taken over all of the vortex filaments in the fluid. Since evaluation of the Biot-Savart integral is very expensive in computer time, the local induction approximation (LIA) is commonly employed (Arms & Hama 1965). In this approximation, the velocity at any point on the vortex filament is given by

$$\vec{v}(\vec{r}) \simeq \frac{\Gamma}{4\pi} \ln(\frac{R_{eff}}{a_0})(\vec{s}' \otimes \vec{s}'') \tag{2}$$

where $'$ denotes differentiation by arclength, a_0 is the core radius, and R_{eff} is an arbitrary length scale. In this project, we choose $R_{eff} = 8R$, where R is the local radius of curvature of the filament. This choice gives the correct velocity for vortex rings (Glaberson & Donnelly 1986). The LIA is only valid if the Biot-Savart integral is dominated by the local region $\vec{s} \simeq \vec{r}$. A practical rule of thumb is that the LIA is not applicable if 'non-local' sections of the vortex filament approach within a

distance of one R. Note that the logarithmic term in Eq. 2 prevents us from non-dimensionalizing the equation of motion unless the logarithmic term is considered constant. In this project, we have allowed the logarithmic term to vary and have, therefore, not non-dimensionalized the equations.

A major difficulty in applying the results of superfluid turbulence experiments to high Reynolds number flows is that helium II is not a pure superfluid but instead behaves as a combination of two fluids, a superfluid and a normal fluid (Wilkes & Betts 1987). The normal fluid is a classical Navier-Stokes fluid with a very small but non-zero viscosity ($\sim 20\mu P$). The quantum excitations which form the normal fluid are scattered by the superfluid vortices, allowing momentum and energy transfer between the two fluids. This coupling, known as mutual friction (Vinen 1957), is represented as a force per unit length on the vortex filament.

$$\vec{F}_{drag} = \gamma_0(\vec{v}_n - \vec{v}_L) \tag{3}$$

where γ_0 is a temperature dependant parameter, $\vec{v}_n$ is the velocity of the normal fluid, and $\vec{v}_L$ is the velocity of the vortex filament. Including this drag force, the filament velocity is given by

$$\vec{v}_L = \vec{v}_s + \vec{v}_I + \alpha \vec{s}' \otimes (\vec{v}_n - \vec{v}_s - \vec{v}_I) \tag{4}$$

where α is another temperature dependant parameter, $\vec{v}_s$ is the imposed superfluid flow, and $\vec{v}_I$ is the self-induced vortex velocity given by either the Biot-Savart law or the LIA.

In our simulation, superfluid vortex filaments are represented by a series of linked straight vortex segments connected at nodes. The velocity at each node is calculated by Eq. 4 using the LIA and the positions of the nodes are integrated forward in time by an adaptive Runge-Kutta-Fehlberg method.

Experiments in superfluid turbulence (Tough 1982) reveal a wealth of turbulent behavior with four possibly distinct turbulent states characterized by geometrical factors and the relative velocity $(\vec{v}_n - \vec{v}_s)$. Through simulation studies, Schwarz (1988) has developed a theory of homogeneous, isotropic superfluid turbulence. This theory has had mixed success in explaining some of the behavior observed in superfluid turbulence experiments.

A feature which has been neglected in superfluid simulations is the interaction of the vortex filaments with a shear flow (or boundary layer) in the normal flow. In simulations of classical vortex filaments, Aref and Flinchem (1984) have found that an initially linear vortex filament placed in the spanwise direction of an imposed external shear flow is unstable (in the LIA) to small perturbations, developing oscillations which the authors liken to turbulent spots. In a similar study, Leonard (1980) has demonstrated an instability of an array of interacting vortex filaments initially arranged to represent a shear layer. Though these studies involve different couplings of the vortex filament and a shear flow than is present in superfluids, they do suggest that such couplings are dynamically interesting.

2. Accomplishments

The first phase of this project has been to upgrade the simulation code of the author so that the full effects of mutual friction may be accurately included. The most important adaptation was to implement a remeshing algorithm to allow the computational grid to adjust to the shrinking and growing of the vortex filaments. These subroutines compare the length, ℓ, of each vortex element to the local radius of curvature, R, of the vortex filaments. Nodes are added or subtracted from the filament meshing to keep the ratio ℓ/R within set limits. This allows the behavior of the vortex filament to be followed as the length scales evolve over many orders of magnitude. When nodes are added to the filament meshing, I have found that the new nodes must be interpolated using splines of at least third order so that the second derivative (corresponding to curvature) is modeled continuously along the filament. If lower degree interpolation is used, artificial curvature fluctuations are introduced which affect the vortex dynamics. It is possible that fourth order interpolation may be necessary to avoid artificial discontinuities in the torsion of the filament. This question is currently being examined.

The physical situation under study at the present time is channel flow of superfluids. We assume that the normal fluid is in laminar channel flow

$$v_n = \frac{3}{2} v_{avg} (1 - (\frac{z}{a})^2) \tag{5}$$

where a is the half-width of the channel, and that the superfluid has a constant velocity v_s. In the simulations discussed in this report, the superfluid velocity is chosen so that the net superfluid and normal fluid flow through the channel are equal, $v_s = v_{avg}$. The vortex behavior that we have observed should not depend qualitatively on the magnitude of v_s. The flow is in the positive y direction, the x axis is spanwise to the flow, and the z axis is normal to the channel boundaries. We initialize the simulation with a small vortex half-ring attached to the lower wall. The ring lies in the x-z plane and is oriented against the flow. The initial radius of the ring is $10^{-1}a$. We find that the final shape of the vortex filament is independent of the initial size of the vortex ring, provided that the initial radius is larger than a small value dependant upon v_s. Since rings are unlikely to be generated with small radii (Schwarz 1990), this limitation is unimportant here. The vortex ring evolves into a horseshoe shape (Figures 1 and 2) with a length longer than the channel height (Figure 3). This horseshoe vortex propagates against the direction of the external flow with little or no change in shape or size. The coupling between the superfluid vortex and the normal fluid boundary layer causes a boundary layer behavior to appear in the superfluid. The existence of these long vortex filaments may play a crucial role in the initiation of superfluid turbulence.

3. Future work

The immediate future phase of this project is to examine the dynamics of the horseshoe vortex filament. Of particular interest is the process which transports energy from the boundary, where mutual friction is causing growth, to the tip of

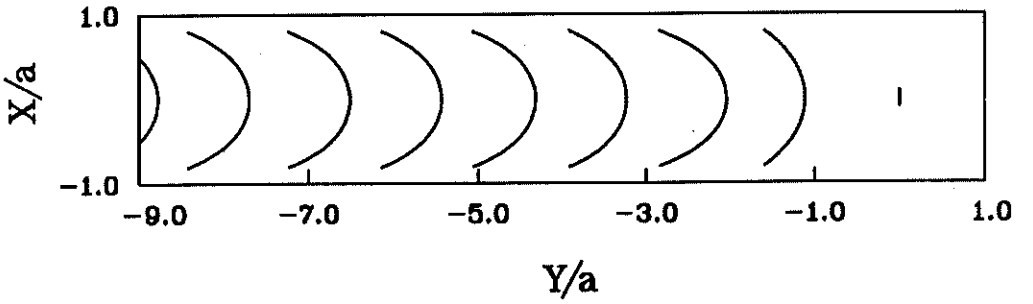

FIGURE 1. Instantaneous configurations of the vortex filament in the $X-Y$ plane as the filament evolves. The time evolution is from right to left.

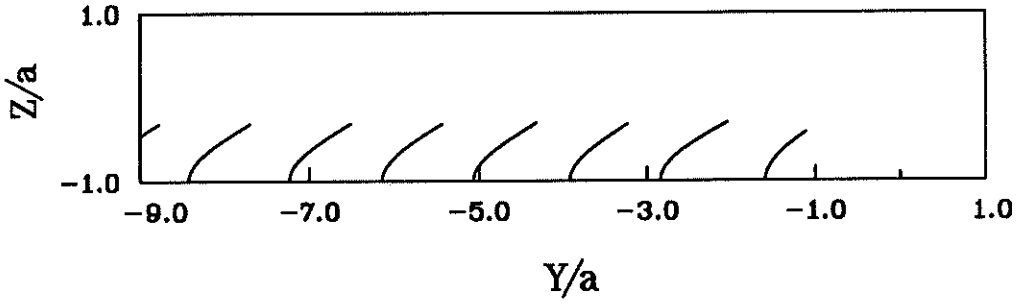

FIGURE 2. Instantaneous configurations in the $Y-Z$ plane.

the vortex, where mutual friction causes the vortex filament to shrink. How is this energy balance maintained to form a vortex with constant length and shape? And very importantly, does this balance break down at higher external flow rates, causing unlimited growth of the vortex filament?

A problem which must be addressed is the possibly non-negligible interaction of a vortex filament of this shape with the solid boundary, represented by an image vortex. In this situation, the local induction approximation may not be sufficient, and full Biot-Savart calculations may be necessary.

In the less immediate future, interactions of these horseshoe vortices will be studied, including merger of vortices and the possible formation of regular arrays of these vortices as is seen in classical fluids (Herbert 1988). It will be necessary to use full Biot-Savart calculations in these simulations.

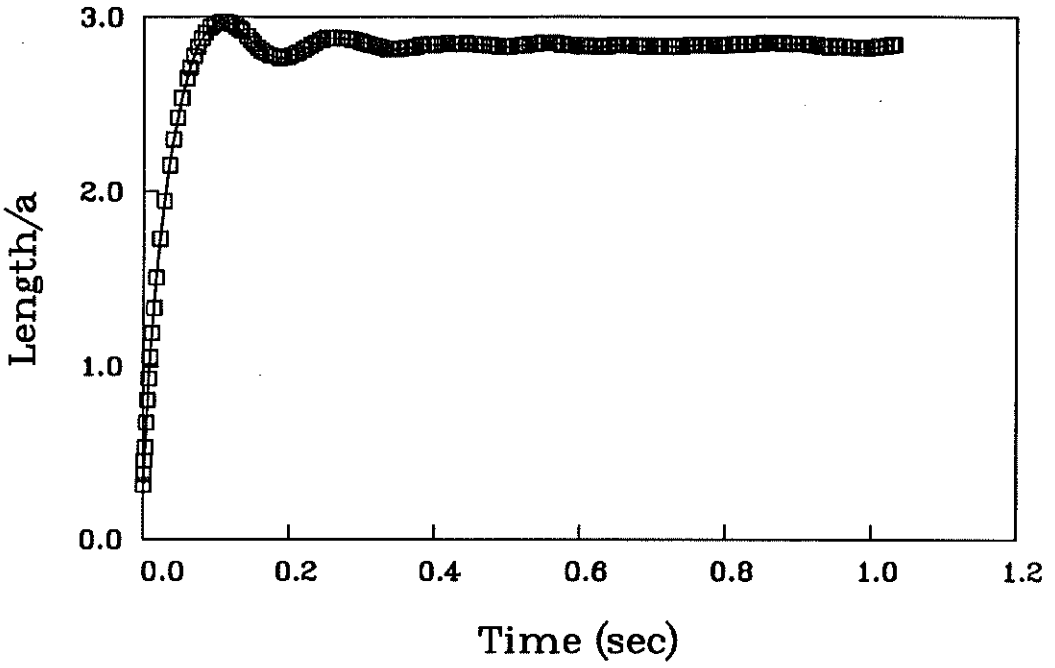

FIGURE 3. Total length of the vortex filament. These results were taken from a simulation with $a = 10^{-2}$ cm and $v_{avg} = 5.0$ cm/sec.

REFERENCES

AREF, H., & FLINCHEM, E. P. 1984 Dynamics of a Vortex Filament in a Shear Flow. *J. Fluid Mech.* **148**, 477-497.

ARMS, R. J., & HAMA, F. R. 1965 Localized-Induction Concept on a Curved Vortex and Motion of an Elliptic Vortex Ring. *Phys. of Fluids.* **8**, 553-559.

GLABERSON, W. I., & DONNELLY, R. J. 1986 Structure, Distributions and Dynamics of Vortices in Helium II. *Prog. in Low Temp. Phy.* **9**, 1-142.

HERBERT, T. 1988 Secondary Instability of Boundary Layers. *Ann. Rev. Fluid Mech.* **20**, 487-526.

SCHWARZ, K. W. 1988 Three-Dimensional Vortex Dynamics in Superfluid He^4 : Homogeneous Superfluid Turbulence. *Phys. Rev. B.* **38**, 2398-2417.

SCHWARZ, K. W. 1990 Phase Slip and Turbulence in Superfluid He^4 : A Vortex Mill That Works. *Phys. Rev. Lett.* **64**, 1130-1133.

TOUGH, J. T. 1982 Superfluid Turbulence. *Prog. in Low Temp. Phys.* **8**, 133-219.

VINEN, W. F. 1957 Mutual Friction in a Heat Current in Liquid Helium II: III. Theory of the Mutual Friction. *Proc. Roy. Soc.* **A242**, 493-515.

WILKS, J. & BETTS, D. S. 1987 *An Introduction to Liquid Helium.* Oxford Science Publications